

Di-hadron and Tri-hadron correlation and Mach-like cone structure in AMPT model

Y. G. Ma^a, G.L. Ma^{a,b}, S. Zhang^{a,b}, X.Z. Cai^a, J.H. Chen^{a,b}, Z.J. He^a, H.Z. Huang^c, J.L. Long^a, W.Q. Shen^a, X.H. Shi^{a,b}, J.X. Zuo^{a,b}

^a Shanghai Institute of Applied Physics, Chinese Academy of Sciences, Shanghai 201800, China,

^b Graduate School of the Chinese Academy of Sciences, Beijing 100080, China,

^c University of California, Los Angeles, CA90095, USA

Abstract. In a framework of a multi-phase transport model with both partonic and hadronic interactions, azimuthal correlations between trigger particles and associated scattering particles in Au + Au collisions at $\sqrt{s_{NN}} = 200$ GeV/c have been studied by the mixing-event technique. The Mach-like structure has been observed in correlation function for central collisions. It is shown that the Mach-like structure is basically born in the partonic process and further developed in hadronic rescattering process. However, hadronic rescattering alone cannot reproduce the amplitude of Mach-like cone on away side, therefore partonic cascade process is necessary to describe the amplitude of Mach-like cone on away side in experiment. In addition, three-particle correlations have been investigated in central Au + Au collisions with the AMPT model, and the results support the conclusion that partonic cascade processes enhance the opening angle of Mach-like cone structures.

Keywords: QGP, AMPT, parton cascade, hadronic rescattering, Mach cone

PACS: 25.75.-q

1. Introduction

The strong suppression of high- p_T particle yield [1] and the disappearance of one jet in back-to-back jet correlation [2] have been observed in Au + Au central collisions at $\sqrt{s_{NN}} = 200$ GeV/c, which can be interpreted by jet quenching mechanism [3]. On the other hand, the loss energy will be redistributed in the soft p_T region [4, 5, 6, 7]. These soft associated particles which carry the loss energy have been reconstructed via two-particle angular correlation of charged particles in STAR experiment [8], which will constrain models for the description of production mechanisms of high p_T particles, and may shed light on the underlying energy loss

mechanisms and the degree of equilibration of jet products in the medium.

The interesting Mach-like structure has been observed recently in two-particle correlation function in Au + Au collisions at $\sqrt{s_{NN}} = 200$ GeV/c [9, 10, 11]. Corresponding theoretical studies have just started with many new ideas. For instance, it was proposed that a Mach shock wave will happen when the jet travels faster than sound in the medium [12, 13, 14, 15, 16]; the Mach-like structure can also be produced with a Cherenkov radiation model [17]; it was attributed to medium dragging effect in Ref. [18].

In this work, we shall study two-particle and three-particle correlations between trigger particle and associated particle(s) and investigate strange Mach-like structure by using a dynamical transport model: a multi-phase transport model (AMPT) [19]. We applied mixing-event technique to AMPT results as people made the analysis for RHIC data and reproduced two-particle and three-particle correlations with AMPT model. It is found that both parton cascade and hadronic rescattering can produce the apparent associated particle correlation as well as Mach-like structure. But the pure hadronic rescattering mechanism can not reproduce the amplitude of Mach-like cone on away side, therefore parton cascade process seems indispensable.

2. Model Introduction

AMPT model [19] is a hybrid model which consists of four main components: the initial condition, partonic interactions, the conversion from partonic matter into hadronic matter and hadronic interactions. The initial condition, which includes the spatial and momentum distributions of minijet partons and soft string excitation, are obtained from the HIJING model [3]. Excitation of strings will melt strings into partons. Scatterings among partons are modelled by Zhang's parton cascade model (ZPC) [20], which at present includes only two-body scattering with cross section obtained from the pQCD with screening mass. In the default AMPT model [21] partons are recombined with their parent strings when they stop interaction, and the resulting strings are converted to hadrons by using a Lund string fragmentation model [22]. In the AMPT model with string melting [23], a simple quark coalescence model is used to combine partons into hadrons. Dynamics of the subsequent hadronic matter is then described by A Relativistic Transport (ART) model [24]. Details of the AMPT model can be found in a recent review [19]. It has been shown that in previous studies [23] the partonic effect could not be neglected and a string melting AMPT is much more appropriate than the default AMPT when the energy density is much higher than the critical density for the pQCD phase transition [19, 23, 25]. In the present work, the parton interaction cross section in AMPT model with string melting is 10mb.

3. Two-particle Correlation Analysis

3.1. Analysis Method

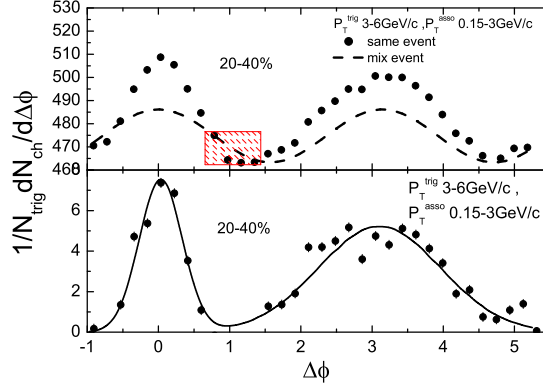


Fig. 1. (a): The associated hadron $\Delta\phi$ distribution for the trigger hadrons with $3 < p_T^{trig} < 6$ GeV/c and the associated hadrons with $0.15 < p_T^{assoc} < 3$ GeV/c (circles) where the background (dash line) is not subtracted for 200 GeV/c Au + Au collisions at 20-40% centrality within AMPT model. The dash area is the region of ZYAM normalization (see texts for detail); (b): The associated hadron $\Delta\phi$ distribution where the background has been subtracted by mixing-event technique, the solid line is its two-Gaussian fit.

In order to reproduce the soft (or hard) associated-hadron correlations, we use the mixing-event technique in our analysis. Two kinds of p_T window cuts for trigger and associated particles are used, one is $3 < p_T^{trig} < 6$ GeV/c and $0.15 < p_T^{assoc} < 3$ GeV/c (we call it as "soft" associated hadrons since the soft particles are dominated), another is $2.5 < p_T^{trig} < 4$ GeV/c and $1.0 < p_T^{assoc} < 2.5$ GeV/c (we call it as "hard" associated hadrons since there are more hard particles than the previous "soft" component). Both trigger and associated particles are selected with pseudo-rapidity window $|\eta| < 1.0$. In the same events, the correlation pairs of the associated particles with trigger particles are accumulated to obtain $\Delta\phi = \phi - \phi_{trig}$ distributions. In order to remove the background which is expected to mainly come from the effect of elliptic flow [8, 10], so-called mixing-event method is applied to simulate its background. In this method, we mixed two events which have very close centrality into a new mixing event, and extracted $\Delta\phi$ distribution which is regarded as the respective background. When subtracting the background from the same events, ZYAM (zero yield at minimum) assumption is adopted as did in experimental analysis [10]. Figure 1 gives us the associated hadron $\Delta\phi$

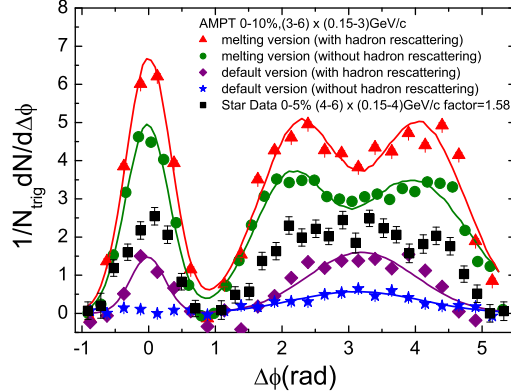


Fig. 2. Soft scattered associated hadron $\Delta\phi$ correlations for the trigger hadrons with $3.0 < p_T^{trig} < 6.0$ GeV/c and the associated hadrons with $0.15 < p_T^{assoc} < 3.0$ GeV/c in most central Au + Au at $\sqrt{s_{NN}} = 200$ GeV/c in AMPT model. Triangles: AMPT melting version (later we just call as melting) after hadronic rescattering; circles: melting before hadronic rescattering; diamonds: AMPT default version (later we just call as default) after hadronic rescattering; stars: default before hadronic rescattering; squares: experimental data from Ref [8] where $4.0 < p_T^{trig} < 6.0$ GeV/c and $0.15 < p_T^{assoc} < 4.0$ GeV/c is taken.

distributions for the trigger hadrons with $3 < p_T^{trig} < 6$ GeV/c and the associated hadrons with $0.15 < p_T^{assoc} < 3$ GeV/c before and after subtracting the background in 200 GeV/c Au + Au collisions at 20-40% centrality within AMPT model.

3.2. Results and Discussions

In order to increase the statistical amount of trigger particles in our calculation, we set p_T range for trigger particles to $3 < p_T^{trig} < 6$ GeV/c and for associated particles to $0.15 < p_T^{assoc} < 3$ GeV/c, and pseudo-rapidity range to $|\eta| < 1.0$ both for trigger and associated particles in our analysis. Both trigger and associated particles are selected with $|\eta| < 1.0$. Figure. 2 presents the soft scattered associated hadron $\Delta\phi$ correlations in most central Au + Au collisions at $\sqrt{s_{NN}}=200$ GeV/c under different conditions. In order to compare our results with experimental data which give the correlations among associated charged hadrons, the experimental data are multiplied by a factor of 1.58 to account for the contribution from neutral hadrons [8, 26]. From the figure, we can see that the hadronic rescattering increases Mach-like $\Delta\phi$ correlations not only for the melting AMPT but also for the Default AMPT. In the melting AMPT, there are very strong Mach-like correlations before

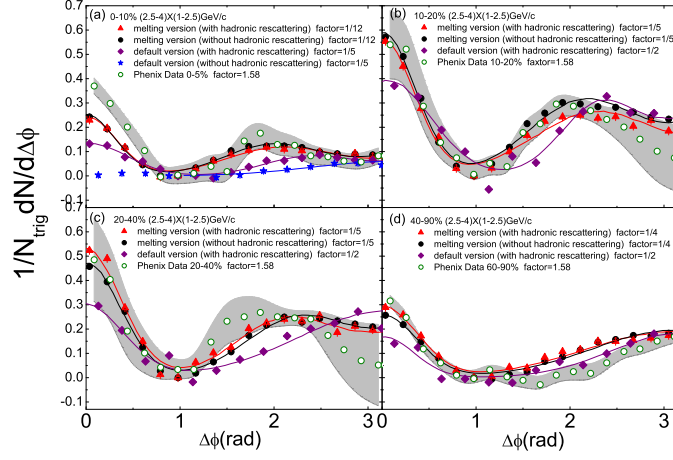


Fig. 3. Hard scattered associated hadron $\Delta\phi$ correlations in Au + Au at 200 GeV/c at different centralities for correlated hadrons with $2.5 < p_T^{trig} < 4.0$ GeV/c and $1.0 < p_T^{assoc} < 2.5$ GeV/c in AMPT model. Triangles: melting after hadronic rescattering; Full circles: melting before hadronic rescattering; Diamonds: default after hadronic rescattering; Stars: default before hadronic rescattering; Open circles: experimental data from Ref. [10]; Hatched areas give the experimental uncertainty.

hadronic rescattering, which indicates that Mach-like structure has been formed in parton cascade process.

For hard scattered associated particles ($2.5 < p_T^{trig} < 4.0$ GeV/c and $1.0 < p_T^{assoc} < 2.5$ GeV/c), Figure 3 shows $\Delta\phi$ correlations in 200 GeV/c Au + Au at different centralities in different conditions. (Note that here our p_T cut is the same as PHENIX cut, But $|\eta|$ cut: $|\eta| < 1.0$ in our model is different from $|\eta| < 0.35$ at PHENIX to increase the statistics in our simulations.) It was found that the effect on $\Delta\phi$ correlations from hadronic rescattering is much smaller than soft scattered associated particles, which may indicate that fewer hard associated hadrons are from hadronic rescattering. In addition, Mach-like structures are observed on away sides in both melting AMPT and default AMPT. However we should point out that in the default AMPT the Mach-like structures can only be observed after hadronic rescattering. For the comparison with the data, the Melting AMPT gives more reasonable splitting between two Mach-like peak in away side. It indicates that partonic interaction is more important to describe the Mach-like structure.

4. Three-particle Correlation Analysis

4.1. Analysis Method

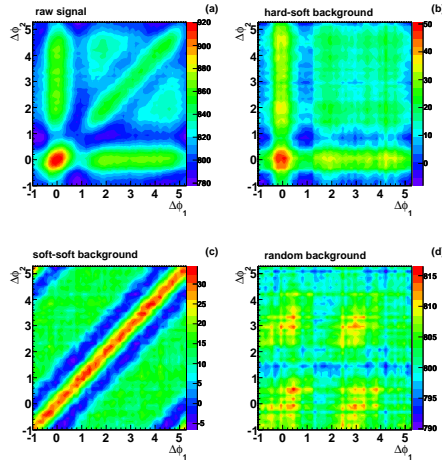


Fig. 4. Three-particle correlations in the 10% most central 200 GeV/c Au + Au collisions (with string melting and hadron rescattering scenario). (a) Raw signal. (b) Hard-soft background. (c) Soft-soft background. (d) Random background.

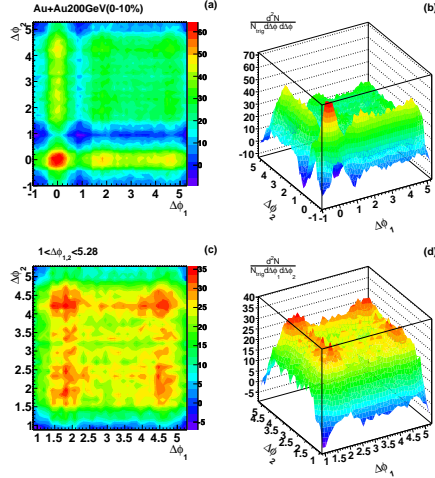


Fig. 5. Background subtracted 3-particle correlations in the 10% most central 200 GeV/c Au + Au collisions (with string melting and after hadron rescattering). (a) and (b): Background subtracted 3-particle correlations ($-1 < \Delta\phi_{1,2} < 5.28$). (c) and (d): Segmental Background subtracted 3-particle correlations ($1 < \Delta\phi_{1,2} < 5.28$).

The mixing-event technique is used in our three-particle correlation analysis. Only hard p_T window cut for trigger and associated particles is selected as $2.5 < p_T^{trig} < 4$ GeV/c and $1.0 < p_T^{assoc} < 2.5$ GeV/c in the analysis. Both trigger and associated particles are selected with pseudo-rapidity window $|\eta| < 1.0$. In the same events, raw 3-particle correlations in $\Delta\phi_1 = \phi_1 - \phi_{trig}$ and $\Delta\phi_2 = \phi_2 - \phi_{trig}$ are accumulated. The figure 4(a) show raw 3-particle correlations in the 10% most central Au+Au at 200 GeV/c collisions with string melting and after hadron rescattering. Three background contributions are expected in raw signal. The first one is a trigger-associated pair combined with a background associated particle, which was reproduce by mixing trigger-associated pairs with another false associated particle that from another events (Figure 4(b)). We call it hard-soft background. The second one is a associated particle pair combined with a background trigger particle, which was reproduce by mixing associated particle pairs with another false trigger

particle that from another events (Figure 4(c)). We call it soft-soft background. The last one is a random background, which are produce by mixing trigger particle and two associated particles respectively from three different events (Figure 4(d)). When subtracting the background from the same events, we normalize the strip of $0.8 < |\Delta\phi_{1,2}| < 1.2$ to zero. Figure 5 (a) and (b) give background subtracted three-particle correlations in the 10% most central 200GeV/c Au+Au collisions with string melting and hadronic rescattering mechanism. In order to see the 3-particle correlations among trigger particle and two away-side associated particles on away side, the zoom-in segmental 3-particle correlations ($1 < \Delta\phi_{1,2} < 5.28$) are shown in figure 5 (c) and (d).

4.2. Results and Discussions

In panel (c) of figure 5, three interesting regions will be investigated. The first one is 'center' region ($|\Delta\phi_{1,2} - \pi| < 0.8$) where three-particle correlations mainly come from trigger particle and two associated particles in the center of away side. The second one is 'deflected' region ($|\Delta\phi_{1,2} - (\pi \pm 1)| < 0.8$) where three-particle correlations reflect three-particle correlations among trigger particle and two associated particle in one same cone of away side and are expected to be due to the sum of away-side jets deflected by radial flow. The third one is 'cone' region ($|\Delta\phi_1 - (\pi \pm 1)| < 0.8$ and $|\Delta\phi_2 - (\pi \mp 1)| < 0.8$) where it gives three-particle correlations among trigger particle and two associated particles from two different cones of away side. It was predicted that 'cone' correlations may be caused by Mach shockwave effect.

It was observed that all 'center', 'deflected' and 'cone' three-particle correlations exist in most central Au+Au collisions at $\sqrt{s_{NN}} = 200$ GeV/c (0-10% centrality) under melting AMPT version after hadronic rescattering. It indicates that these three different mechanisms may contribute to three-particle correlation in most central Au+Au collisions, i.e. one part of associated particles go through reaction system, one part of associated particles are deflected, and other part of associated particles produce Mach-like correlations.

5. Summary

In summary, the origin of the Mach-like correlation for soft or hard scattered associated particles was investigated in the framework of the AMPT model which includes two dynamical processes, namely parton cascade and hadronic rescattering. By comparing the different two-particle and three-particle correlation calculation results before or after hadronic rescattering, with or without string melting mechanism, it is argued that the associated particle correlation and Mach-like structure have been formed before hadronic rescattering, which indicates that these kinds of correlations are born in the partonic process and are further developed in later-on hadronic rescattering process. In our work, it is shown that hadron rescattering mechanism can produce the associated particle correlation, but it can not give big enough splitting for away-side Mach-like peaks in confronting with experimental

data. In this context, the parton cascade mechanism is essential for describing experimental Mach-like structure.

This work was supported in part by the Shanghai Development Foundation for Science and Technology under Grant Numbers 05XD14021, the National Natural Science Foundation of China under Grant No 10328259, 10135030, 10535010.

References

1. S.S. Adler et al. (PHENIX Collaboration), Phys. Rev. Lett. **91**, 072303 (2003); J. Adams et al. (STAR Collaboration), Phys. Rev. Lett. **91**, 072304 (2003).
2. C. Adler et al. (STAR Collaboration), Phys. Rev. Lett. **90**, 082302 (2003).
3. M. Gyulassy and X.-N. Wang, Comput. Phys. Commun. **83**, 307 (1994).
4. S. Pal and S. Pratt, Phys. Lett. B **574**, 21 (2003).
5. C. A. Salgado and U.A. Wiedemann, Phys. Rev. Lett. **93**, 042301 (2004).
6. I. Vitev, Phys.Lett. B **630**, 78 (2005).
7. X.-N. Wang, Phys. Lett. B **579**, 299 (2004).
8. J. Adams et al. (STAR Collaboration), Phys. Rev. Lett. **95**, 152301 (2005).
9. J. G. Ulery [STAR Collaboration], Nucl.Phys. A **774**, 581 (2006).
10. S. S. Adler et al. [PHENIX Collaboration], Phys. Rev. Lett. **97**, 052301 (2006).
11. Jiangyong Jia [PHENIX Collaboration], arXiv:nucl-ex/0510019.
12. H. Stöcker, Nucl. Phys. A **750**, 121 (2005).
13. J. Casalderrey-Solana, E. V. Shuryak, D. Teaney, J. Phys. Conf. Ser. **27**, 22 (2005).
14. J. Ruppert, B.Müller, Phys. Lett. B **618**, 123 (2005) .
15. T. Renk and J. Ruppert, Phys.Rev. C **73**, 011901 (2006).
16. A. K. Chaudhuri, Ulrich W. Heinz, Phys. Rev. Lett. **97**, 062301 (2006).
17. V. Koch, A. Majumder, Xin-Nian Wang, Phys. Rev. Lett. **96**, 172302 (2006).
18. N. Armesto, C. A. Salgado, Urs. A. Wiedemann, Phys.Rev. C **72**, 064910 (2005).
19. Z. W. Lin et al., Phys. Rev. C **72**, 064901 (2005).
20. B. Zhang, Comput. Phys. Commun. **109**, 193 (1998).
21. B. Zhang, C. M. Ko et al., Phys. Rev. C **61**, 067901 (2000).
22. B. Andersson, G. Gustafson et al., Phys. Rep. **97**, 31 (1983).
23. Z.W. Lin et al., Phys. Rev. C **65**, 034904 (2002).
24. B. A. Li and C. M. Ko, Phys. Rev. C **52**, 2037 (1995).
25. J. H. Chen, Y. G. Ma, G. L. Ma et al., arXiv:nucl-th/0504055, to be published in Phys. Rev. C.
26. J. Adams et al. (STAR Collaboration), Phys. Rev. Lett. **92**, 112301 (2004); S.S. Adler et al. (PHENIX Collaboration), Phys. Rev. C **69**, 034909 (2004).